

CONTRIBUTIONS TO RELIABILITY MODELING AND EVALUATION OF PROTECTIVE STRUCTURE SUBSYSTEMS IN URBAN MEDIUM VOLTAGE ELECTRICITY NETWORKS

LĂZĂROIU G., MIHĂESCU L., PÎȘĂ I., PRISECARU T., POP E., TOADER M.M.,
 NICULESCU B., MĂRUNȚĂLU O., STAN N.A.
 University POLITEHNICA of Bucharest
glazarioiu@yahoo.com

Abstract - This paper is structured in five activities, each of which has a great importance in conducting the research. In the first part are made experimental determinations of solid biomass for energy characteristic features. The following two parts shows the theoretical mathematics numerical and modelling of the adsorption processes of hydrogen respectively hydrogen burning of solid biomass. Finally the last two parts shows the experimental testing of solid biomass combustion.

Keywords: solid biomass, renewable sources, sorghum, hydrogen combustion jet

1. INTRODUCTION

Fossil represents 80,3% over primary energy consumed in the world, but only 23% of this amount is used in the energy sector. SRE-E may have a fundamental role in managing the challenges driven by climate change, environmental degradation and energy security. In the EU, all 27 Member States have implemented a range of support mechanisms for the promotion of electricity from renewable sources, to support the introduction of RES-E market, the quota of RES-E in the European Union. Intermediate goal for the EU-27 is 12% renewable energy by 2010, and a share of electricity from renewable sources by 21%. By 2020, renewable energy must arrive at the rate of 20%. Many of the EU-27 countries have made important progress in promoting renewable energy sources in the energy mix. However, there remain many obstacles and the need for greater efforts to meet its goal for the year 2020. Until now, the share of electricity from renewable sources is not defined for 2020, but "plan for renewable Energy" of the EU Commission (2007) involves the odds of SRE-E in 2020 of 42.8%-34.2, depending on the scenario. Currently, all 27 Member States have implemented 27 different national support schemes [1], [5]. RES-E is an essential element for the development of a sustainable energy mix, and can contribute to energy policy objectives in two ways: *Reducing CO2 and other emissions; Development of new technologies.*

2. EXPERIMENTS FOR THE CHARACTERISTICS OF SOLID BIOMASS ENERGY

2.1. Biomass resources and energy potential

Biomass is the third-largest source of primary energy in the world, after coal and oil. The main source of biomass is wood. Alongside wood there is a wide variety of resources, such as:

- energy crops;
- residue (wood from tree medicine is applied) straw and stalks of grain, other residues from processing of food (sugar cane, tea, coffee, nuts, olives);
- waste and by-products (waste from wood processing: shavings, sawdust, paper, waste organic fraction of municipal waste, waste vegetable oils and animal fats);
- methane captured from landfills, from plants for

Biomass energy high potential agricultural residues and residues include activities related to the forest. Residues from forest-related activities (excluding wood) represents 65% of the energy potential of biomass while 33% comes from agricultural crops residues. Wooded acreage in the EU covers 137 million hectares, and the agricultural area is 175 million hectares. These resources can provide, after cover requirements of food and paper, 11% of the total annual energy demand in the EU. New resources in the form of crops for energy purposes made, can provide annually 2 J, of which about 60% in the form of solid biomass for heat and electricity production and 40% for bio-fuels. The recent reforms of the EU's agricultural crops for energy encourage by offering grants (45 Euro/ha), thus ensuring an area of 1.5 million hectares [6].

In Romania, about 90% of the wood fire and 55% of the wood waste can be found in the Carpathians and Subcarpathians. About 54% of the agricultural waste can be found in the plains and southern Moldavia. About 52% of the biogas is found in the southern plains and west plains. Of the total area of Romania, agriculture uses about 70% of wood resources. The entire agricultural area for grain it uses 66%, 14% and feed crops for technical crops 13%. According to an autonomous public corporation ROMSILVA annual output of lumber can be reached at 18 million cubic in 2020, mostly being used in construction and industry.

2.2. General properties of physical, chemical and energetical of solid biomass

Solid biomass is similar to coal, but coal is different in terms of content of organic and inorganic materials, calorific value and physical properties. Compared with coal, biomass has generally less carbon, aluminum and iron and more oxygen, potassium, silica and has a lower calorific value, water content, density and low friability. The burning of biomass combustion process involves changing in any installation due to the composition of the biomass, especially volatile content. The spray combustion of biomass is dominated by volatilization and combustion in gaseous phase as opposed to burning coal, which is dominated by coke formation and oxidation of gas-solid. Elemental analysis (composition) of biomass is the main form of definition of energy properties and influences ecological and efficient use of biomass. Elemental analysis for determination requires very expensive equipment and highly trained personnel. Technical analysis, which is a complement, only requires standard laboratory equipment and can be done by staff without special preparation. Technical analysis, which is a complement, only requires standard laboratory equipment and can be done by staff without special preparation. The presence of inorganic compounds in bio-fuels affect the combustion process as well as the composition of the ash. The concentration of heavy metals (particularly the Cd and Zn) in the ashes of biomass increases with decreasing temperature and precipitation particle size. This effect is independent of bio-fuel use. High concentrations of K, Na, Cl, and flying ash in biomass influences than the reactions that can occur in the boiler, the combustion gases are subjected to a temperature gradient considerably with chemical reactions, phase change and precipitation [2], [3].

2.3. Description of fuels laboratory

Currently, the lab has a full line for fuel preparation and analysis, starting with proximate/technical analysis of a solid fuel and continuing with ultimate/elemental analysis of solid and liquid fuels.

2.3.1. Proximate (technical) analysis of the fuel

Proximate analysis of a fuel consist in determination of moisture, volatile matter, ash and fixed carbon content of the fuel. For moisture content determination, The Fuel Lab is equipped with a POL-EKO SLN53ECO oven with natural convection range ED. The oven has an ATP technology with preheating chamber which assures temperature accuracy and reproducible results; temperature range: 5°C above ambient - 300°C; DS controller with integrated timer 0-99 hours; digital temperature setting with an accuracy of 1°C. The fuel laboratory from Thermal Research Centre is also equipped with a furnace Nabertherm LE14/11 model, to determine the volatile fraction, fixed carbon and inert solid fuels. The furnace has five ramps of heating and a working temperature up to 1100 ° C [7].



Fig. 1.1 Oven POL-EKO SLN53ECO

2.3.2. Ultimate (elemental) analysis

For quantitative analysis of C, H, N, S, O content of a fuel, the laboratory is equipped with an Elemental Analyzer COSTECH ECS 4010 – CHNS-O and a high precision Sartorius analytical balance.

Operating modes of the analyzer: CHNS, CHN, CNS, CN, N, S, A. Fields of detection: C: 0.004 - 30 mg abs; H: 0.002 - 3 mg abs; N: 0.001 - 10 mg abs; S: 0.005 - 6 mg abs; A: 0.005 - 2 mg abs. Standard deviation: 0.1% abs (CHN simultaneously, 4-5 mg sample). Operating Temperature: 950-1200⁰C.



Fig. 2.1 Analyzer COSTECH ECS 4010 – CHNS-O

2.3.3. Energetic characteristics determinations for biomass in UPB – ETCN Fuel Laboratory

The energetical characteristics for categories of biomass that will be tested for most appropriate combustion technologies, has been determined in UPB – ETCN Fuel Laboratory. We have considered the following categories of biomass: wood waste, straw, grain, reeds, energetic and sweet sorghum; composite biomass briquettes.

a. The energetical characstics of wood waste

		Wood waste	Variation with wood essence		
			Beech	Pine	Spruce
Carbon	C % (dry mass)	50	49,3	51	50,9
Hydrogen	H % (dry mass)	6,2	5,8	6,1	5,8
Oxygen	O % (dry mass)	43	43,9	42,3	41,3
Nitrogen	N % (dry mass)	0,3	0,22	0,1	0,39
Sulf	S % (dry mass)	0,05	0,04	0,02	0,06
Clorine	Cl % (dry mass)	0,02	0,01	0,01	0,03
Cenușă	A % (dry mass)	1	0,7	0,5	1,5
Volatile	V % (dry mass)	81	83,8	81,8	80

b. The energetic characteristics of wheat and rye straw

Characteristici	Yellow straw	Grey straw
Moisture content, W_i^1	10-20	10-20
Volatile matter, V^1	≥ 70	> 70
Ash content, A^1	4	3
Carbon, C^1	42	43
Hydrogen H^1	5	5,2
Oxygen O^1	37	38
Chloride %	0,75	0,2
Nitrogen N^1	0,35	0,41
Sulph combustibile S_c^1	0,16	0,13
Low heating value Q_i^1	14,4	15

c. The energetic characteristics of straw and composite briquette

Nr. crt.	Fuel	Elemental analysis [%]						
		C	H	N	S	O	A	W
1	Acacia wood	49,6	6,0	0,9	0,1	33,8	4,20	5,4
2	Reed briquette	48,4	5,5	0,6	0,0	31,2	7,30	7,0
3	Sawdust briquette	50,0	5,9	1,8	0,0	33,6	2,60	6,0
4	Sawdust briquette 50% + stalks 50%	46,1	5,5	0,4	0,0	38,0	3,30	6,7
5	Sawdust briquette 50% + straw 50%	48,0	5,8	0,5	0,0	36,1	4,40	5,2
6	Sawdust briquette 25% + stalks 75%	48,2	5,9	0,6	0,0	34,5	3,40	7,5
7	Sawdust briquette 25% + straw 75%	48,5	5,7	0,7	0,0	36,4	1,40	7,3

d. The energetic characteristics of sorghum

SORGHUM 1– Hybrid Porumbeni 4-leaf, panicles and stem;
 SORGHUM 2 - Hybrid F135-ST Fundulea (sweet sorghum)- leaf, panicles and stem

	Wt	C	H	N
SORGHUM 1	%	%	%	%
Leaf	9.08	44.7	5.8	2
Panicles	14.2	44.8	5.7	1.4
Stem	43.5	22.1	7.1	0.2
SORGHUM 2	%	%	%	%
Leaf	11.66	45.4	5.8	1.1
Panicles	12.45	44	6.1	1.7
Stem	38.18	27.9	7.8	0.2

	S	O	A	Q_i
SORGHUM 1	%	%	%	kJ/kg
Leaf	-	28	10.42	17850
Panicles	-	28.5	5.4	17600
Stem	-	25.8	1.3	10900
SORGHUM 2	%	%	%	kJ/kg
Leaf	-	27.5	8.54	18070
Panicles	-	32.9	2.85	17300
Stem	-	23.6	2.32	14000

3. THEORETICAL MATHEMATICAL AND NUMERIC MODELING OF PROCESSES FOR ABSORPTION OF HYDROGEN BY THE SOLID BIOMASS

Using hydrogen in solid biomass burning is intended to improve conditions of ignition and burning speed. It is proposed, in particular in the form of biomass briquettes of cereal straw or sawdust. Modeling research of hydrogen diffusion in porous system of solid biomass. It took into account the biomass briquetting solid from maxi-size lighter until the pellet. Briquetting system creates a set of similar coal pores.

3.1. Mathematical model for the diffusion of a gas in the pores of a solid fuel.

A mathematical model has been development for gas diffusion in a porous system and based on it a numerical simulation for hydrogen absorption gas been carried out.

The equation which describes hydrogen diffusion in the pores of a renewable fuel is:

$$D_i \cdot \frac{d^2C}{dx^2} + q = 0 \tag{3.1}$$

Equation (3.1) can be written as follows:

$$\frac{d^2C}{dx^2} = -\frac{q}{D_i} \tag{3.2}$$

Integration of equation (3.2) leads to:

$$\frac{dC}{dx} = -\frac{q}{D_i} \cdot x + C_1 \tag{3.3}$$

The solution of equation (3.3) is:

$$C = -\frac{q}{2 \cdot D_i} \cdot x^2 + C_1 \cdot x + C_2 \tag{3.4}$$

The boundary conditions needed in order to determine the constants C_1 and C_2 are:

$$x = 0; C = C_s \rightarrow C_2 = C_s \tag{3.5}$$

where, C_s is hydrogen concentration on the particle surface.

Finally, the equation which describes the variation of hydrogen concentration inside the pores can be written as:

$$C = -\frac{q}{2 \cdot D_i} \cdot x^2 - \frac{q}{D_i} \cdot l \cdot x + C_s = C_s - \frac{q}{D_i} \cdot l \cdot x - \frac{q}{2 \cdot D_i} \cdot x^2 \tag{3.6}$$

$$C_s = q \cdot \tau \tag{3.7}$$

Based on equation (3.6) the hydrogen concentration at a certain pore length l can be calculated as follows:

$$C_l = C_s - \frac{q}{D_i} \cdot l^2 - \frac{q}{2 \cdot D_i} \cdot l^2 \tag{3.8}$$

Further, equation (3.7) can be written:

$$C_l = q \cdot \tau - \frac{3}{2} \cdot \frac{q}{D_i} \cdot l^2 = q \cdot \left(\tau - \frac{3}{2} \cdot \frac{l^2}{D_i} \right) \tag{3.9}$$

Time needed for the absorption process can be calculated with:

$$\tau \geq \frac{3}{2} \cdot \frac{l^2}{D_i} \tag{3.10}$$

The concentration variation inside the pore can be computed as follows:

$$C_m = \frac{\int_0^l \left(C_s - \frac{q}{D_i} \cdot l \cdot x - \frac{q}{2 \cdot D_i} \cdot x^2 \right) dx}{l} = \frac{\left(C_s \cdot x - \frac{q}{D_i} \cdot \frac{l \cdot x^2}{2} - \frac{q}{2 \cdot D_i} \cdot \frac{x^3}{3} \right) \Big|_0^l}{l} \quad (3.11)$$

$$C_m = C_s - \frac{q}{2 \cdot D_i} \cdot l^2 - \frac{q}{2 \cdot D_i} \cdot \frac{l^2}{3} = C_s - \frac{2}{3} \cdot \frac{q}{D_i} \cdot l^2 \quad (3.12)$$

Using equation (2.12) the quantity of absorbed hydrogen can be calculated with:

$$Q = V \cdot C_m \cdot S_i \cdot \varepsilon \quad (3.13)$$

where, C_m is the average concentration.

3.2. Results of mathematical model

The conditions in which the mathematical modeling has been developed are presented in next table.

The results obtained based on the mathematical model and the program developed in MathCAD have been presented graphically in Figures 3.1....3.8.

Conditions for mathematical model

No.	Parameter	Value
1	Hydrogen flux q [kg/(m ³ ·s)]	(1;1.5;2)·10 ⁻⁶
2	The pore length l [m]	(1;2;3;4;5;6;7; 8;9;10)·10 ⁻⁷
3	The particle volume V [m ³]	(1;2;5;10;20)·10 ⁻³
4	The internal pore surface S_i [m ² /m ³]	100;150
5	Relative pore depth during reaction ε [m]	0.497

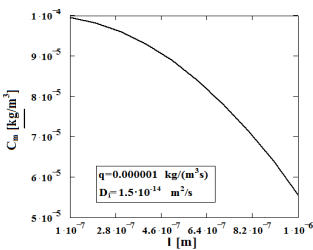


Fig. 3.1

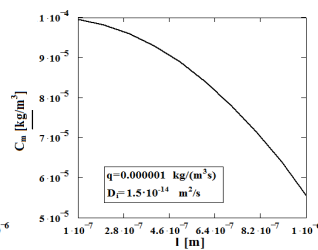


Fig. 3.2

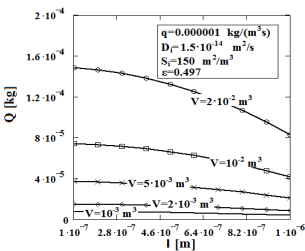


Fig. 3.3

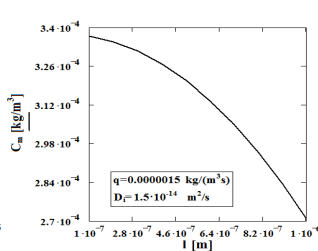


Fig. 3.4

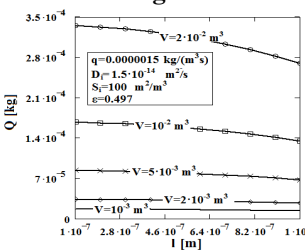


Fig. 3.5

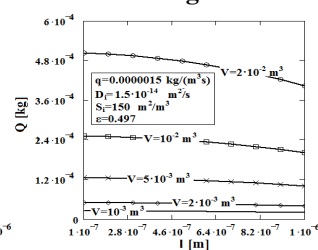


Fig. 3.6

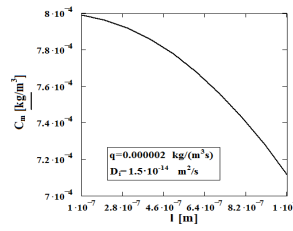


Fig. 3.7

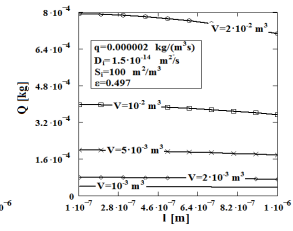


Fig. 3.8

4. THEORETICAL MATHEMATICAL AND NUMERIC MODELING OF COMBUSTION PROCESSES OF SOLID BIOMASS UNDER HYDROGEN INLET FLOW

4.1. Modeling by thermography of the sorghum combustion process

Sorghum is a productive plant, unpretentious to soil fertility or drought and involves minimal cost for cultivation and processing. It is a plant that produces no loss even the wastes being profitable. Sorghum cultivation on large areas, in addition to the economic and ecological benefits, is solving partially, the air pollution problem (1 ha of sorghum absorbs annually from the atmosphere up to 50-55 tons of carbon dioxide, while the hardwood absorbs 16 t / ha / year and cereals 3-10 t / ha / year). In the context of the Kyoto Protocol, Romania is likely to have significant gains by cultivating large areas with this plant [4].

4.2. Research objectives

Thermal Research Centre from the University Polytechnica of Bucharest is endowed with adequate equipment that allows us to study the sorghum as fuel, in terms of its energy recovery. We analyzed two types of sorghum, by stem, panicle and leaves, which will be referred to as SORGHUM 3 and SORGHUM 4. Mass weight of these three components cannot be determined precisely yet, even by statistics, so it was decided to analyze separately the three components of the plant. For these two types of sorghum elemental analysis has been carried out. The possibilities for direct combustion and the ash softening temperature have been defined. Analysis has been performed with an Elemental analyzer, COSTECH ECS 4010 type. The usual analysis was performed in two steps: first, the quantitative determination of carbon, hydrogen, sulfur, nitrogen content have been done and in the second step, the amount of oxygen has been determined.

Elemental analysis of sorghum 3

Sorghum 3	Wt	C	H	N	S
	%	%	%	%	%
leaf	9.53	46.93	6.09	2.1	-
panicles	14.91	47.04	5.985	1.47	-
stem	45.67	23.2	7.45	0.21	-

Sorghum 3	O	A	Q _{I an}	Q _{I ex}
	%	%	kJ/kg	kJ/kg
leaf	29.4	10.94	18739	18761
panicles	29.92	5.67	18474	18508
stem	27.09	1.36	11445	11404

Elemental analysis of sorghum 4

Sorghum 4	Wt	C	H	N	S
	%	%	%	%	%
leaf	12.24	47.67	6.09	1.15	-
panicles	13.07	46.2	6.4	1.78	-
stem	40.08	29.29	8.19	0.21	-

Sorghum 4	O	A	Q _{I an}	Q _{I ex}
	%	%	kJ/kg	kJ/kg
leaf	28.87	8.96	18977	19002
panicles	34.54	2.9	18165	18198
stem	24.78	2.43	14659	14612

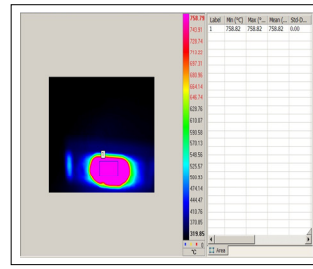


Figure 4.3. Spectrum evolution obtained by recording with IR camera, the temperatures during the combustion process.

Also, the amounts of nitrogen monoxide in the flue gas have been decreased as the temperature of the flame was too small. It has been noticed that if we continue sorghum drying, the results will change. This means that natural drying is not enough. We can consider there was not a combustion process but only a weak gasification, without an adequate contact surfaces between minced sorghum and oxygen.

4.3. Combustion experiment

For combustion tests we considered two cases: the burning of combustible material in bulk form and in the fine minced form. For bulk material combustion a 55 kW boiler has been used. The boiler has been equipped with a liquid fuel burner and solid fuel grate. The bulk material has been introduced into the combustion chamber and the combustion has been primed with liquid fuel burner after which the sorghum combustion took place. For the mincing/ shredding plant special equipment with electrically operated drum was used. The resulted fuel is a material with a mean size of 10 mm. The combustion for shredded fuel has been performed on the 30 kW ERPEK boiler, fully automatic.

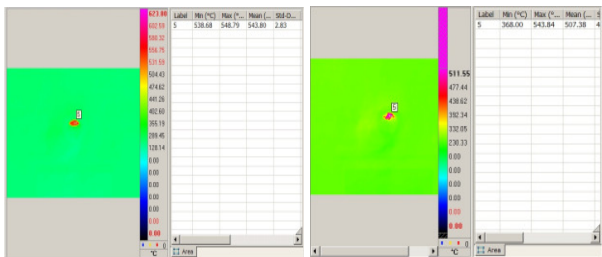


Fig. 4.1 55 kW PIFATI boiler- front view



Fig. 4.2 30kW ERPEK boiler- front view

For gas analysis, two gas analyzers AFRISO Maxilizer and HORIBA PG250 have been used. In Figure 4.3 below, we can see the ignition of the fuel (sorghum) and the flame progress as the temperature increase



5. EXPERIMENTAL TESTS REGARDING BIOMASS COMBUSTION IN AIR AND HYDROGEN JET

Combustion technology under jet air corresponds to the pulverized combustion when the fuel particles are involved in a continuous flow in the outbreak. The feeding fuel of the furnace is done with a special construction to carry out the function of the ignition and the filling of the entire volume of the outbreak.

5.1. Experimental tests regarding biomass combustion in air jet

In principle, an installation to burn sawdust in a pulverized state has the following components: a fuel bunker, for an autonomy range of 4 to 6 hours, a pneumatic system to feed the sawdust to the burner, a primary, secondary and tertiary air fan and also a flue gas fan. The burner ensures a flow of 0.5 kg/s of sawdust, having a 15500 kJ/kg to 19000 kJ/kg calculation calorific heat value.

The elemental analysis of the sawdust was:

$$C^i = 44,8\%, \quad H^i = 4,8\%, \quad O^i = 33,2\%,$$

$$S_c^i = 0\%, \quad N^i = 1\%, \quad A^i = 5,6\%, \quad W_i^i = 10,6\%$$

A complete automatized boiler, with moving fire grate has the following auxiliary electrically acted:

- Combustion feeder;
- Acting moving grate;
- Ash and slag discharge;
- Air fan;
- Gas fan.

As a result the members of Thermotechnics and thermal equipments department of University „Politehnica” of Bucharest proposed the construction of a burner for sawdust and wood slivers, in a modulating conception, starting from 600 kW thermal power.

The burner was designed by UPB members and carried out by ICEMENERG SA with the next characteristics:

- Thermal power: max 500 kW;
- Reduced weight (under 50kg);
- Self-supporting construction (all subassemblies are welded with the central channel of primary agent, which sustains the entire construction);
- Radial dimensions that permit to implement the burner in the furnace (furnace embrasure $\varnothing 168$).

The thermal normal operation of the fluids is in the next domain:

- The primary agent temperature (60-90°C); this value is imposed by the humidity of the sawdust at the entrance of the feeding system and the temperature of primary air;
- The primary air temperature is between 150-200°C depending on thermal charge. To avoid an accidental ignition of the sawdust (of the emitted volatile substances of sawdust in contact with the heated primary air) it can be used a dilution of the oxygen concentration by recirculating burnt gases;
- The secondary air temperature, 150-220°C;
- The tertiary air temperature, 150-220°C.

The characteristics of burner working are:

1. The thermal support combustible quota

• Gas volume/ sawdust mass: $q_B = B_g / B$, where: B_g [m^3_N/h]- the natural gas flow capacity used as thermal support, B [kg/h]-the sawdust flow capacity. The calculus of sawdust flow capacity was $B = 80$ kg/h;

• Thermal quota $q_B^* = \frac{B_g \cdot Q_g}{B \cdot Q_i^i}$, where: Q_g -the calorific heat value of the thermal support gas ($Q_g=37500$ kJ/ m^3_N), Q_i^i - the calorific heat value of the sawdust.

2. The pneumatic transportation capacity of sawdust from the stoking bunker to the burner, defined by volumetric concentration of the sawdust in the air transport $c = \frac{B}{\dot{V}_a}$, where: \dot{V}_a is the air flow capacity for pneumatic transportation. As mass ratio, the sawdust concentration for transportation is: $c^* = \frac{B}{\dot{V}_a \cdot \rho_a}$, where:

ρ_a [kg/ m^3]-the density of the air for sawdust transportation (rectified for the real temperature).

3. The thermal charge of the burner embrasure

$q_a = \frac{B \cdot Q_i^i}{S_a}$, where: Q_i^i [kJ/kg]- the calorific heat value of sawdust, S_a [m^2]- the area of embrasure (for the embrasure diameter of 168mm, the area is 0.022 m^2).

4. The thermal charge of the furnace volume compared with the project one is: $q_v = \frac{B \cdot Q_i^i}{V_f}$, where:

V_f - the active furnace volume. The designed thermal charge of the furnace volume has the value $q_v = 40$ kW/ m^3 .

5.1.1. Experimental results

The experimental tests aimed at the finding of ignition capacity and efficient burning (in pulverized state) in an energetic medium power installation. The tests were made in the pilot furnace of 2 MW_t of UPB,

Thermotechnics and thermal equipments Department, where it was implemented the new burner for wood slivers and multiple swirling jets of 500kW thermal power. The furnace start was made with a gas burner of 40 m^3_N/h natural gas flow capacity. The calorific heat value was $Q_i^i = 19860$ kJ/kg .

Figure 4.2 present the flame in the furnace, visualized from the back visiting door or the furnace, using a non IR digital camera. It is remarkable a strong intensity and radiation of the flame, similar to pit coal flame.



Fig.5.1. The general aspect of the flame evolution

5.2. Experimental tests regarding biomass combustion in air and hydrogen jet

HRG injection before the burner has been proposed in order to support the ignition process. HRG is obtained through water electrolysis and it represents a mixture of atoms and radicals (H, OH, O, HO₂) having the low heat value of hydrogen (10760 kJ/ Nm³). The HRG is produced by a generator having a maximum volume flow rate of 4 Nm³/h [6].

The burner ensures a flow of 0.5 kg/s of sawdust, having a 14115 kJ/kg calculation calorific heat value. The elemental analysis of the sawdust was:

$C^i = 42,7\%$, $H^i = 4,7\%$, $O^i = 36,3\%$,
 $S_c^i = 0\%$, $N^i = 1\%$, $A^i = 5,5\%$, $W_t^i = 9,8\%$

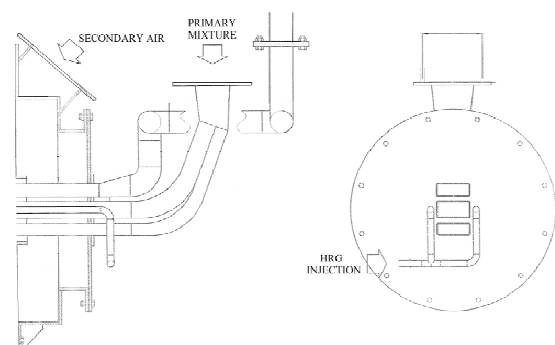


Fig. 5.2 HRG Injection system

5.2.1. Experimental results here:

The experimental tests aimed to find the ignition capacity and burning efficiency (in pulverized state) in an energetic medium power installation.

The tests were made in the pilot furnace of 2 MW_t of UPB, Thermodynamics, engines, thermal and refrigeration equipments Department, where it was

implemented the new burner for wood slivers and multiple swirling jets of 620kW thermal power.

The technology of suspension burning of sawdust with swirling burners makes possible the increase of power from medium to high energy production. So, if the tested burner has a thermal power of 620 kW_t, following the principles to realize it, the power can be increased to 3MW_t for the next burners.

- The thermal support combustible quota. Gas volume/ sawdust mass:

- the maximum value $q_B=0,05 \text{ m}^3_N/\text{kg}$ sawdust;
- the minimum value $q_B=0 \text{ m}^3_N/\text{kg}$ sawdust

- The pneumatic transportation capacity.

The sawdust mass concentration in the transportation air was: $c=0,24 \text{ kg/m}^3$ and $c^*=0,19 \text{ kg/kg}$.

- During the tests, the air excess value were:

$$O_2=1,2-6,6 \text{ \%}; \lambda=1,06-1,45$$

- The carbon monoxide emission was:

$$CO=19,8-43 \text{ mg/m}^3.$$

This value is incontestable lower to that of the layer burning technology. The NO_x emission was:

$$NO_x=375-387 \text{ mg/m}^3.$$

6. EXPERIMENTAL TESTS REGARDING BIOMASS COMBUSTION IN HYDROGEN JET-PHASE 1

6.1. Experimental tests regarding dense biomass combustion in air jet

The research of the combustion of dense biomass is conducted on a 55-kW boiler. A boiler with reduced thermal power, which can supply a residential area or a small commercial area, was chosen. The concept to implement the use of composite fuels in hill and mountain forestry area was the principle of the research.

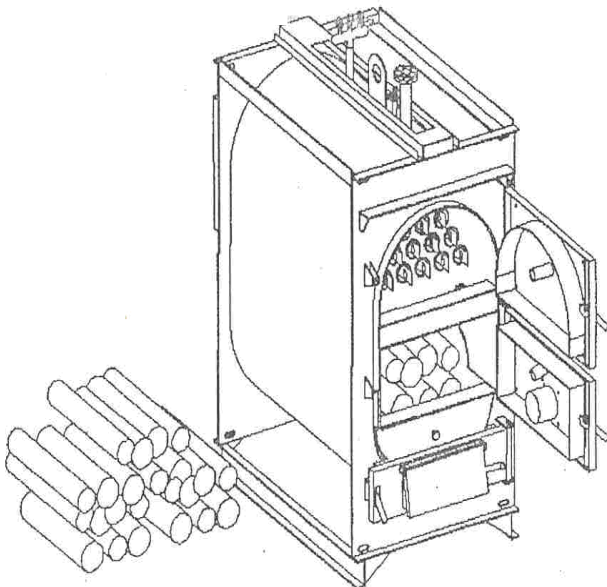


Fig. 6.1 55-kW boiler

6.1.1. Characteristic of 55-kW boiler

The 55-kW test facility boiler has the following dimensions of the furnace: depth $L_f=750 \text{ mm}$; width $l_f=550 \text{ mm}$; height $h_f=600 \text{ mm}$; volume $V_f=0.25 \text{ m}^3$.

The furnace is equipped with a grid with fixed bars, having the dimensions: length $L_g=520 \text{ mm}$; width $l_g=550 \text{ mm}$; bars width $l_b=15 \text{ mm}$; bars spacing $s=15 \text{ mm}$; length of the free space between bars $l_{sl}=360 \text{ mm}$; grid surface $S_g=0.286 \text{ m}^2$; grid active surface $S_{ga}=0.19 \text{ m}^2$. The fuel flow necessary for achieving 55 kW thermal power (P_t) is:

$$B \left[\frac{\text{kg}}{\text{s}} \right] = \frac{P_t}{Q_i^i \cdot \eta}$$

value.

For briquettes composed from dense biomass and wood wastes like sawdust, the low heat value varies between 12500 and 13200 kJ/kg.

Elementary composition of the components and composite from wood biomass

Element	Symbol	M.U.	Wood biomass
Carbon	C ⁱ	%	46.48
Hydrogen	H ⁱ	%	6.10
Oxygen	O ⁱ	%	41.80
Nitrogen	N ⁱ	%	0.63
Sulphur	S ⁱ _c	%	0.00
Ash	A ⁱ	%	1.17
Total humidity	W ⁱ _t	%	3.82

Considering a low heat value 12.700 kJ/kg, the rate of the fuel flow is:

$$B = \frac{55}{12700 \cdot 0.7} = 0,006 \text{ [kg/s]} = 22.2 \text{ [kg/h]} \quad (6.1)$$

Using this value, the operational coefficients for the boiler are:

- total gravimetric load of the grid:

$$q_{gr} = \frac{0.006}{0.286} = 0.021 \text{ [kg/m}^2 \cdot \text{s]};$$

- gravimetric load of the combustion area:

$$q_{gr}^* = \frac{0.006}{0.19} = 0.031 \text{ [kg/m}^2 \cdot \text{s]};$$

- total specific thermal load of the grid:

$$q_{gr} = \frac{0.006 \cdot 12700}{0.286} = 269 \text{ [kW/m}^2 \cdot \text{s]};$$

- specific thermal load of the grid active area:

$$q_{gr} = \frac{6 \cdot 12700}{190} = 400 \text{ [kW/m}^2 \cdot \text{s]};$$

- active section of the grid: 0.346; cooling index of the grid bars: 1.33;

- thermal load of the furnace width:

$$q_l = \frac{B \cdot Q_i^i}{l_f} = \frac{0.6 \cdot 12700}{55} = 140 \text{ [kW/m]};$$

- thermal load of the grid bars width:

$$q_i^* = \frac{B \cdot Q_i^i}{l_f} = \frac{6 \cdot 12700}{275} = 280 \text{ [kW/m]};$$

- thermal load of the furnace volume:

$$q_v = \frac{B \cdot Q_i^i}{V_f} = \frac{6 \cdot 12700}{250} = 305 \text{ [kW/m}^3 \text{]}.$$

6.1.2. Experimental data

Experimental data sheet No 1

No	Operating characteristic	M.U.	Measurement			
			1	2	3	4
1	thermal load	kW	50	50	50	49
2	combustible	kg/h	17	16.9	17	17
3	slag	kg/h	0.88	0.9	0.9	0.89
4	ash	kg/h	2.8	2.75	2.8	2.75
5	stack temperature	°C	160	161	160	162
6	water flow	kg/h	810	812	811	812
7	inlet water temperature (t_i)	°C	8	8	8	8
8	exit water temperature	°C	59	61	61	61
9	CO ₂ emission	%	3.9	4.0	3.8	3.9
10	SO ₂ emission	ppm	70	72	72	70
11	NO emission	ppm	30	30	27	26
12	NO ₂ emission	ppm	0	10	0	0
13	NO _x total	ppm	30	40	27	26
14	CO emission	%	0.24	0.16	0.2	0.18
15	furnace air excess, λ_f		3.2	3.1	3.2	3.3
16	stack air excess, λ_{co}		3.4	3.4	3.37	3.4
17	oxygen in the stack exhaust gases (O ₂)	%	14.8	14.6	14.6	14.7
18	air temperature	°C	15	17	16.5	17
19	average ambient temperature	°C	2	2	2	2
20	indirect efficiency		76.7	77.1	77.2	78.1

Experimental data sheet No 2

No	Operating characteristic	M.U.	Measurement			
			1	2	3	4
1	thermal load	kW	45	44.9	45	45
2	combustible	kg/h	15.2	15.2	15.2	14.9
3	slag	kg/h	0.86	0.86	0.88	0.9
4	ash	kg/h	2.60	2.61	2.60	2.61
5	stack	°C	159	157	157	157
6	water flow	kg/h	730	726	769	728
7	inlet water	°C	8	8	8	8
8	exit water	°C	61	59	60	60.5
9	CO ₂ emission	%	3.9	3.89	3.9	3.91
10	SO ₂ emission	ppm	71	72	68	72
11	NO emission	ppm	30	32	31	32
12	NO ₂ emission	ppm	14	15	18	17
13	NO _x total	ppm	44	47	49	49
14	CO emission	%	0.16	0.16	0.13	0.14
15	furnace air		3.3	3.55	3.3	3.3
16	stack air		3.5	3.55	3.5	3.49
17	oxygen in the	%	14.9	14.9	14.79	14.9
18	air	°C	14	15	15	15
19	average	°C	-2	-2	-2	-2
20	indirect		76.5	76.5	76.6	76.6

The taste data values for the 50 kW load have indicated:

- a quantity of slag evacuated below the grid of 5.5-6.5%; the volume of the slag retaining room of 0.5 × 0.54 × 0.6 = 0.162 m³ allows an evacuation at 6 h;

- the disturbance of the mixture layer dense biomass is occurring at a period of 2-3 h;
- the temperature of the fuel layer during the combustion was of 850°C;
- the temperature of the stack flue gas was below 160°C;
- the air excess of the stack flue gas had optimal values for the combustion technology in fixed layer below 3.5;
- the measured efficiency is over 76%;
- the pollutants emissions are reduced. If a reference air excess characterized by an oxygen percentage in the exhausted gases of 11% is considered, the CO emissions are below 500 mg/m³, NO_x emissions below 185 mg/m³ and SO₂ emissions below 300 mg/Nm³.

The performances of the nominal operation load were kept both for 45 kW (90%) ad 40 kW (80%) loads. For a boiler load below 60%, a reduction with 4-5% of the efficiency was observed.

Thermal power is: $P_t = 4.18 \cdot D_a \cdot (t_e - t_i)$ [KW], where D_a is water flow, kg/s; t_e – outlet temperature of the boiler water, °C;

Representative samples of flow slag and ash were collected and tasted in laboratory boiler. As results were obtained: $C_{sl} = 18\%$; $C_{ash} = 5\%$ (combustible material in slag and ash); $a_{sl} = 0.06$; $a_{ash} = 1 - 0.06 = 0.94$ (retaining degree under the shape of slag and ash).

After computation, the values for the percentage heat losses are: loss through incomplete combustion from the mechanical point of view, $q_m = 2.46$; loss through incomplete combustion from the chemical point of view, $q_{ch} = 3.57$; loss through the enthalpy of the residuum evacuated from the furnace, $q_{rf} = 0.056\%$.

For a temperature of the stack exhausted gases of 160°C and an air excess $\lambda_{ev} = 3.4$, the heat percentage loss at evacuation resulted $q_{ev} = 19.3\%$.

For computing the heat losses through incomplete chemical combustion, the CO emission had the average value of 0.18%, and the volume of the dry exhausted gases of $V_{eg} = 22.56 \text{ m}^3_N/\text{kg}$. On statistical basis, the heat loss towards the ambient is determined $q_{ex} = 1.5$.

$$\eta = 100 - (2.46 + 3.5715 + 0.056 + 19.3) = 73.12\% \quad (6.1)$$

$$q_m + q_{ch} + q_{rf} = 7.58\% \quad (6.2)$$

The efficiency computed only using the heat percentage losses at the stack exhausted gas will be:

$$\eta = 100 - 19.3 = 80.7 \quad (6.3)$$

The efficiency measured with the gas analyzer was $\eta = 77.2$. The percentage error is:

$$\Delta\eta = \frac{80.7 - 73.12}{80.7} \cdot 100 = 9.4\% \quad (6.4)$$

6.1.3. Numerical modeling results

For geometric modeling of the 55-kW experimental boiler 164 483 cells were used, grouped as: 147 538 cells with tetrahedron form and 16 945 cells with hexagon form.

For the turbulence model, the Spalart-Almaras model was used. This model is specific for the reduced turbulences (the combustion of the mixture combustible

particles on the grid in a fixed layer conducts to a reduced turbulence).

For the radiation model, the ‘6-fluxes model’ was used. For the radiation model, the physical measures imposed are: average absorption, $\epsilon_p = 0.35 \text{ m}^{-1}$; average particles spreading coefficient, 0; metallic wall emission factor $\epsilon = 0.8$. For the coke particles drawn in suspension by the combustion gases the size of $4.38 \times 10^{-4} \text{ m}$ was chosen.

For simulating the composite combustible granulation the real size of the briquettes with diameter of 40 mm and height of 40 mm was used.

The results highlighted that the combustion area of the furnace is sufficiently large to ensure a good combustion. Thus, the CO emission on the furnace end was 0.03 kg/kg. For an oxygen concentration of approximately 7% within the combustion gases, the corrected emission of CO at the flame ending was $\text{CO} = 970 \text{ mg/m}^3 \text{ N}$.

The numerical modeling result, through combustion performances, indicates as future perspective the possibility to reduce the air excess and to increase the layer and flame temperature. It must be mentioned that this boiler has cast iron grid and thus the operation with high temperatures within the combustion area are allowed.

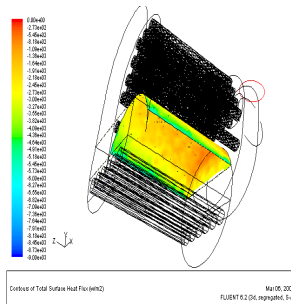


Fig. 6.2 Heat flux on the furnace top

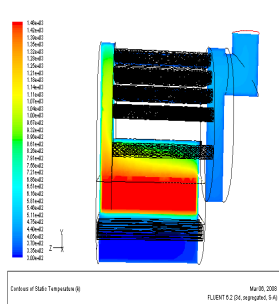


Fig. 6.3 Temperature field for the furnace

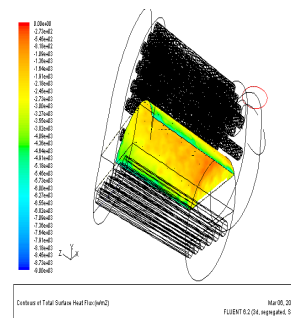


Fig. 6.4 Heat flux distribution for the smoke pipe walls

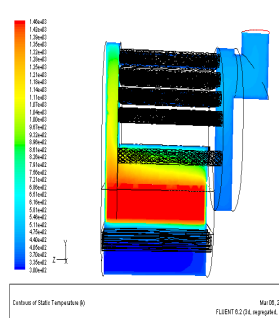


Fig. 6.5 Temperatures distribution for the furnace area

6.2. Experimental tests regarding dense biomass combustion in hydrogen and air jet

The utilization of hydrogen to the biomass combustion has the role to improve the combustion conditions and to increase the reaction rate. Furthermore, this fact influences the CO and NO_x concentrations.

6.2.1. Experimental data

A mathematical model has been development for gas diffusion in a porous system and based on it a numerical simulation for hydrogen absorption gas been carried out.

The equation which describes hydrogen diffusion in the pores of a renewable fuel is:

$$D_i \cdot \frac{d^2 C}{dx^2} + q = 0 \Rightarrow \frac{d^2 C}{dx^2} = -\frac{q}{D_i} \quad (6.5)$$

The boundary conditions needed in order to determine the constants C_1 and C_2 are:

$$x = 0; C = C_s \rightarrow C_2 = C_s \quad (6.6)$$

where, C_s is hydrogen concentration on the particle surface.

Finally, the equation which describes the variation of hydrogen concentration inside the pores can be written as:

$$C = -\frac{q}{2 \cdot D_i} \cdot x^2 - \frac{q}{D_i} \cdot l \cdot x + C_s = C_s - \frac{q}{D_i} \cdot l \cdot x - \frac{q}{2 \cdot D_i} \cdot x^2 \quad (6.7)$$

$C_s = q \cdot \tau$, q - hydrogen flux; τ - time.

The hydrogen concentration at a certain pore length l can be calculated as follows:

$$C_l = C_s - \frac{q}{D_i} \cdot l^2 - \frac{q}{2 \cdot D_i} \cdot l^2 \quad (6.8)$$

$$C_l = q \cdot \tau - \frac{3}{2} \cdot \frac{q}{D_i} \cdot l^2 = q \cdot \left(\tau - \frac{3}{2} \cdot \frac{l^2}{D_i} \right) \quad (6.9)$$

The concentration variation inside the pore can be computed as follows:

$$C_m = \int_0^l \left(C_s - \frac{q}{D_i} \cdot l \cdot x - \frac{q}{2 \cdot D_i} \cdot x^2 \right) dx = \left(C_s \cdot x - \frac{q}{D_i} \cdot l \cdot \frac{x^2}{2} - \frac{q}{2 \cdot D_i} \cdot \frac{x^3}{3} \right) \Big|_0^l$$

$$C_m = C_s - \frac{q}{2 \cdot D_i} \cdot l^2 - \frac{q}{2 \cdot D_i} \cdot \frac{l^2}{3} = C_s - \frac{2}{3} \cdot \frac{q}{D_i} \cdot l^2 \quad (6.10)$$

$$Q = V \cdot C_m \cdot S_i \cdot \epsilon, \text{ kg.} \quad (6.11)$$

6.2.2. Results of mathematical model

Conditions for mathematical model

No.	Parameter	Value
1	Hydrogen flux q [kg/(m ³ ·s)]	(1;1.5;2) · 10 ⁻⁶
2	The pore length l [m]	(1;2;3;4;5;6;7;8;9;10) · 10 ⁻⁷
3	The particle volume V [m ³]	(1;2;5;10;20) · 10 ⁻³
4	The internal pore surface S_i [m ² /m ³]	100;150
5	Relative pore depth during reaction ϵ [m]	0.497

The results obtained based on the mathematical model and the program developed in MathCAD have been presented graphically in figures 6.6, 6.7 and 6.8.

The absorbed hydrogen quantity decreases with the increase of the pore length. For a given value of the pore length, Q increases with the increase of q . At the same time a bigger particle volume leads to a higher Q value.

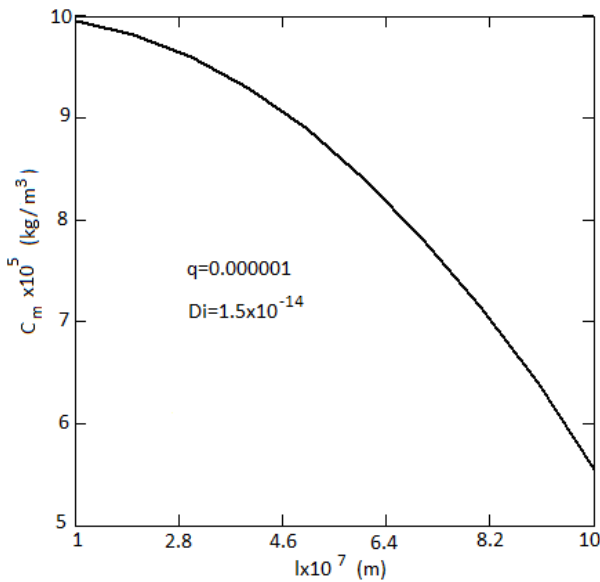


Fig. 6.6 Concentration variation inside the pore in function of pore length

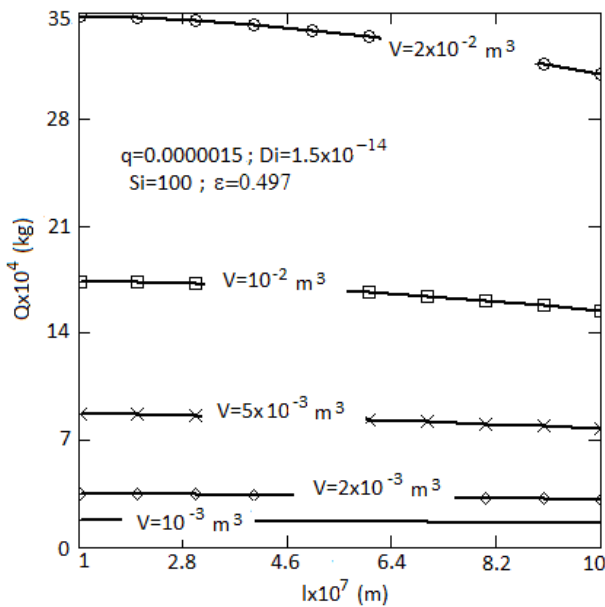


Fig. 6.7 Absorbed hydrogen quantity in function of pore length

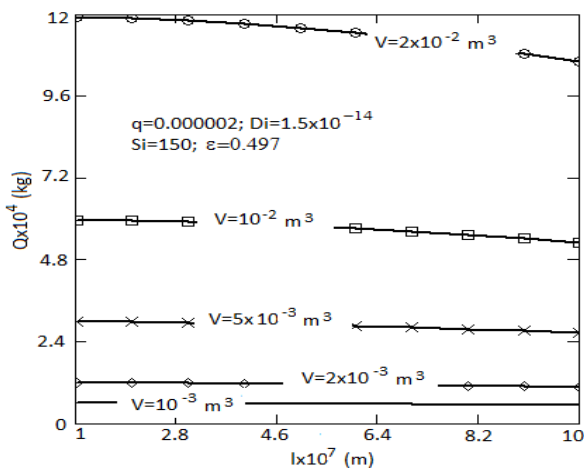


Fig. 6.8 Variation of hydrogen absorbed quantity in function of pore length for different volume values

6.2.3 Experimental work

Experimental researches were done in two phases. First the samples tested (chopped wood, sawdust and energy willow, Figure 6.9) were passed through a stream of hydrogen.

Time was between 0.5 and 25 seconds, depending on particle size. Hydrogen feeding was made from a tank and the samples were placed in a tube (Figure 6.10). More tests were made to obtain sufficient quantities of chopped wood, sawdust or energy willow.

The samples were weighed before and after hydrogen diffusion. Generally, it was found a mass loss of 4-5 %. The explanation may be removing and replacing oxygen from the particle pores by hydrogen which has lower density.

In the second part of researches the samples were burned in a small thermal boiler (20 - 40 kWt).



Fig. 6.9 Samples used in experimental tests



Fig. 6.10 Experimental stand for hydrogen diffusion

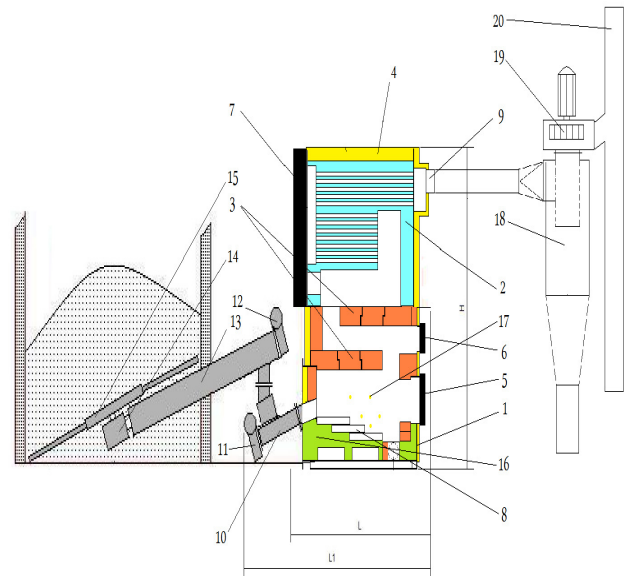


Fig. 6.11 Main components of the biomass boiler

1- furnace; 2- heat exchanger; 3- double vault of refractory cement; 4- wool glass insulation; 5- door for grate cleaning; 6- door for vault cleaning; 7- door for heat exchanger cleaning; 8- mobile grate; 9- flue gasses exhaust; 10- worm-screw supplier; 11- first motor-gear transmission; 12- second motor-gear transmission; 13- worm-screw supplier from the storage; 14- reducing extractor; 15- pan extractor; 16- primary air; 17- secondary air; 18- flue gasses cleaning cyclone; 19- flue gasses fan; 20- chimney.

Biomass type	Parameter	Value
Chpped wood with H ₂	Flame temperature	840°C
	Heat loss, q _{ch}	0.51 %
	CO concentration*	1020 ppm
	SO ₂ concentration*	3-8 ppm
	NO _x concentration*	45-50 ppm
Chpped wood without H ₂	Flame temperature	780°C
	Heat loss, q _{ch}	0.72 %
	CO concentration*	1490 ppm
	SO ₂ concentration*	5-10 ppm
	NO _x concentration*	40-45 ppm
Sawdust with H ₂	Flame temperature	810°C
	Heat loss, q _{ch}	0.63 %
	CO concentration*	1242 ppm
	SO ₂ concentration*	3-5 ppm
	NO _x concentration*	~ 50 ppm
Sawdust without H ₂	Flame temperature	740°C
	Heat loss, q _{ch}	0.74 %
	CO concentration*	1450 ppm
	SO ₂ concentration*	8-10 ppm
	NO _x concentration*	50-55 ppm
Energy willow with H ₂	Flame temperature	823°C
	Heat loss, q _{ch}	0.57 %
	CO concentration*	1174 ppm
	SO ₂ concentration*	6-8 ppm
	NO _x concentration*	40-55 ppm
Energy willow without H ₂	Flame temperature	775°C
	Heat loss, q _{ch}	0.72 %
	CO concentration*	1472 ppm
	SO ₂ concentration*	5-9 ppm
	NO _x concentration*	45-50 ppm

This fact means that the utilization of hydrogen to the biomass combustion improves the combustion conditions and increases the reaction rate. Attempts were made also for pellets, but their porosity being small the hydrogen absorption is insignificant. Next step in our researches is injected directly into the boiler feed system. In this case we use a mixture of hydrogen and helium or hydrogen enriched gas (named HRG) for the safety of researchers. An important issue is the price of producing hydrogen or mixture.

7. CONCLUSION

- The designed burner successfully achieved the rated thermal power 620 kW, for a sawdust flow capacity of 80-85 kg/h and 4 Nm³ HRG. In all these stages the flame had high temperatures, similar to pit coal flame working with. The flame had high brilliancy aspect and filled the entire furnace volume;
- The numerical modeling data of the complex processes within the furnace, containing combustion reactions, heat emitting, heat exchange through radiation and partially convection, flow and pollutant emissions, can be used for

the design of new installations or for instructions for an economic exploitation of these type of installations;

- The good results obtained at the combustion on fixed grids of the dense combustible recommends the enlargement of the combustion researches also on mobile grids, thing that leads to the increase of the thermal power for these boilers;
- Hydrogen injection in porous biomass leads flame temperature increases by about 10 %, and to CO concentration decreases by about 25-30 %. The heat loss q_{ch} decreases by 15-30 %. This fact means that the utilization of hydrogen to the biomass combustion improves the combustion conditions and increases the reaction rate;
- Next step in our researches is direct injection of gas into the boiler feed system. In this case we use a mixture of hydrogen and helium or hydrogen enriched gas (named HRG), for lower costs and for the safety of researchers.

REFERENCES

- [1]. G. Pintilie, M. Moscovici, Interactive European Network for Industrial Crops and their Applications. Forming Part of the IENICA-INFORRM Project. Romanian Report. The Fifth Framework Programme by DG XII, Bucharest, 2004.
- [2]. L. Barbanti, a.o., Sweet and fibre sorghum (*Sorghum bicolor* (L.) Moench), energy crops in the frame of environmental protection from excessive nitrogen loads, European Journal of Agronomy, Vol. 25, Iss. 1, July 2006, pp. 30–39.
- [3]. C.R. Cardoso , a.o., Determination of kinetic parameters and analytical pyrolysis of tobacco waste and sorghum bagasse, Journal of Analytical and Applied Pyrolysis, Vol. 92, Iss. 2, Nov. 2011, pp. 392–400.
- [4]. J. F. González, a.o. , Use of energy crops for domestic heating with a mural boiler, Fuel Processing Technology, Vol. 87, Iss. 8, August 2006, pp 717–726.
- [5]. Velcescu B., Staicu M., The Potential of Romanian Agriculture for Energy Crops, BIOENERGY in EU countries – Current Status and Future Trends, Cluj-Napoca, România, USAMV, May 2011.
- [6]. Pișă Ionel, Lazaroiu Gheorghe, INFLUENCE OF CO-COMBUSTION OF COAL/BIOMASS ON HE CORROSION, Fuel Processing Technology 104, Volume: 104.
- [7]. Ionel Pișă, Corina Radulescu, Lucian Mihaescu, Gheorghe Lazaroiu, Gabriel Negreanu, Simona Zamfir, Danut Vaireanu, EVALUATION OF CORROSIVE EFFECTS IN CO- FIRING PROCESS OF BIOMASS AND COAL, Environmental Engineering and Management Journal, ISSN 1582-9596, November/December 2009 Vol. 8 No. 6.